



CO₂ complexation with cyclodextrins

Cecilie Høgføldt Jessen, Jesper Bendix, Theis Brock Nannestad, Heloisa Bordallo, Martin Jæger Pedersen, Christian Marcus Pedersen and Mikael Bols*

Full Research Paper

[Open Access](#)

Address:
Department of Chemistry & Niels Bohr Institute, University of
Copenhagen, 2100 København Ø, Denmark

Email:
Mikael Bols* - bols@chem.ku.dk

* Corresponding author

Keywords:
carbon dioxide; crystals; cyclodextrin; gas binding

Beilstein J. Org. Chem. **2023**, *19*, 1021–1027.
<https://doi.org/10.3762/bjoc.19.78>

Received: 06 June 2023

Accepted: 11 July 2023

Published: 17 July 2023

Associate Editor: H. Ritter



© 2023 Jessen et al.; licensee Beilstein-Institut.
License and terms: see end of document.

Abstract

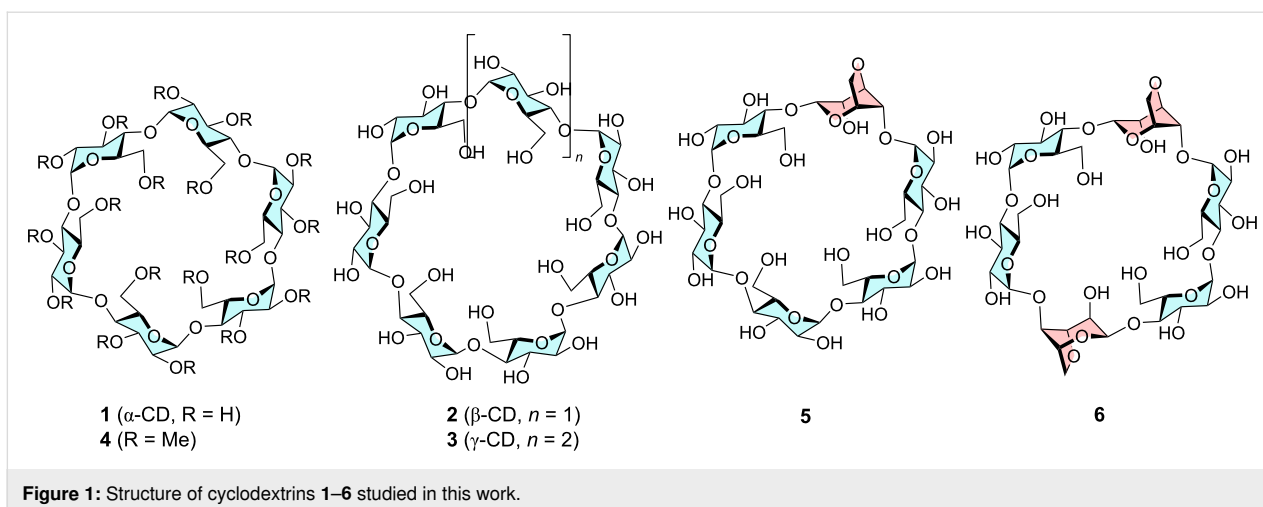
Carbon dioxide (CO₂) emissions from industrial processes, power generation, and transportation contribute significantly to global warming and climate change. Carbon capture and storage (CCS) technologies are essential to reduce these emissions and mitigate the effects of climate change. Cyclodextrins (CDs), cyclic oligosaccharides, are studied as potential CO₂ capture agents due to their unique molecular structures and high selectivity towards CO₂. In this paper we have investigated binding efficiency of a number of cyclodextrins towards CO₂. It is found that the crystal structure of α -cyclodextrin with CO₂ has a 1:1 stoichiometry and that a number of simple and modified cyclodextrins bind CO₂ in water with a K_g of 0.18–1.2 bar⁻¹ (7–35 M⁻¹) with per-*O*-methyl α -cyclodextrin having the highest CO₂ affinity.

Introduction

The concentration of carbon dioxide (CO₂) in the Earth's atmosphere has increased significantly in recent decades [1,2] presumably due to human activity and the extensive burning of fossil fuels. With the ability of CO₂ to absorb energy from sunlight [3], global warming and climate change is expected and serious consequences anticipated. To mitigate the effects of climate change, it is essential to reduce CO₂ emissions from various sources, such as industrial processes, power generation, and transportation. Carbon capture and storage (CCS) technologies are crucial to achieving this goal. CCS technologies involve capturing CO₂ from industrial processes or power plants, transporting it to a storage site, and storing it underground or consuming it by forming polymers [4] or fuels from

CO₂ [5,6]. However, the implementation of CCS technologies faces many challenges, including high costs, energy consumption, and the need for large-scale infrastructure. One of the characteristics of carbon capture technologies that use amines is the formation of a covalent bond to the CO₂ molecule. This bond obviously has to be broken in order to regenerate the material with resulting energy cost [7]. It is therefore logical to explore capture alternatives where CO₂ is captured by non-covalent binding.

Henglein and Cramer showed many years ago that α -cyclodextrin (**1**, Figure 1), when treated with CO₂ under pressure for several days gave crystals with the gas trapped inside [8]. Ac-



According to Cramer only **1** was able to form crystals, while larger cyclodextrins such as **2** and **3** did not. Recently the solid complex of CO_2 and **1** have been studied as a food product additive [9–11]. Anions of **1** in DMSO have been found to have a high capacity for capturing of CO_2 [12]. Being cheap, biodegradable and eco-friendly these carbohydrates might form the basis in an economic CO_2 capture technology. We have therefore studied the binding of CO_2 to simple cyclodextrins to determine binding stoichiometry and affinity. It is found that the crystal structure of α -cyclodextrin with CO_2 has 1:1 stoichiometry and that a number of simple and modified cyclodextrins bind CO_2 in water with a K_g of 0.18–1.2 bar^{-1} (7–35 M^{-1}).

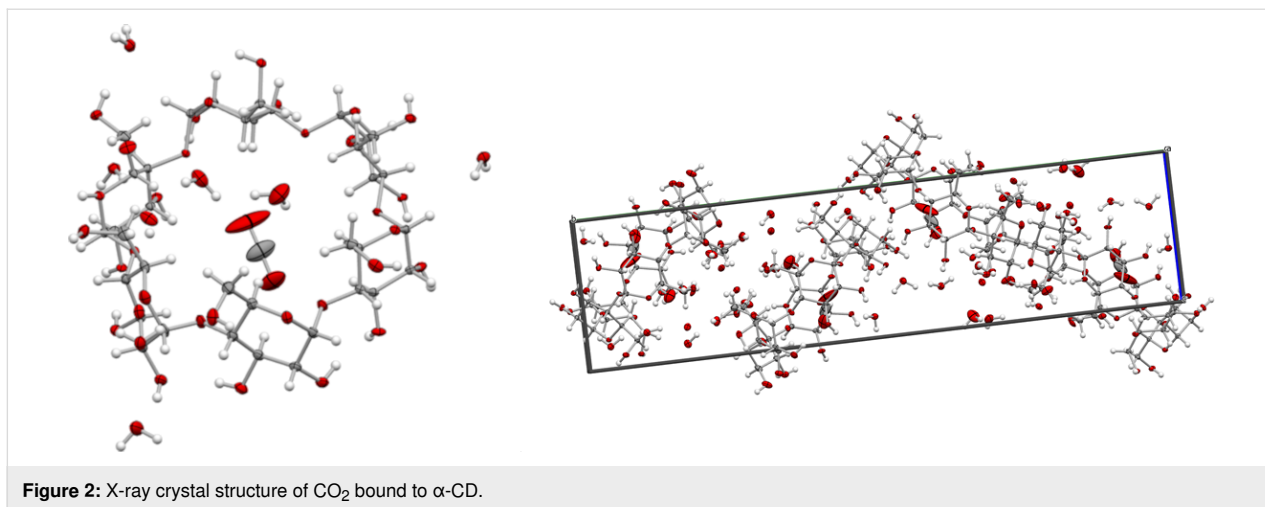
Results and Discussion

When a saturated solution of **1** was treated with CO_2 at a pressure from 6–20 bar in an autoclave for 1–19 days, crystals containing CO_2 were obtained in 16–63% yield (Table 1). The most important factor for getting higher yields was sufficient time for the crystallization, while the pressure was found less important. From the binding constant measured below and the 1:1 stoichiometry ($K_g = 0.18 \text{ bar}^{-1}$, Table 2) we know that 1/2 to 3/4 of the cyclodextrin is filled with CO_2 at the pressures used as

shown in the 5th column of Table 1. As CO_2 is in large excess high crystal yields can be obtained even though the CD cavity is only partially filled, because more CO_2 is bound in solution as crystallization proceeds. When equilibrium is reached as in entries 1–3 (Table 1) the concentration of **1**- CO_2 is 0.04 M which must be the solubility of this complex in water. X-ray crystallography of the crystals showed a 1:1 complex of CO_2 to α -CD with CO_2 bound in the center of the wide, secondary rim of the α -CD cavity (Figure 2). Two of the hydroxymethyl side groups on the primary narrow rim are disordered. The disordering was modeled over two positions for each hydroxymethyl group with one of the positions leading to engagement in hydrogen bonding to water molecules bound at the narrow rim with a combined occupancy of 0.75. Additionally, five fully occupied water molecules are found in the structure one of which is best modeled as split over two positions yielding in total 5.75 mol of water per CO_2 . The hydration is similar to that of native α -CD [13] and that of the krypton inclusion complex which has 5.28 water/Kr [14]. The CO_2 molecule refines with an optimal occupancy of 0.84 and linear geometry ($178.2(6)^\circ$) with C–O bond lengths of 1.138(7) Å/1.146(5) Å. Refinement with full occupancy is also consistent with the diffraction data and yields realistic geometries.

Table 1: The results of crystallization of α -cyclodextrin from water in an atmosphere of CO_2 carried out in a pressure autoclave. $[\text{CD}]_{\text{tot}}$ is the starting concentration of cyclodextrin. $[\text{CD}\cdot\text{CO}_2]/[\text{CD}]_{\text{tot}}$ is the calculated ratio of bound CO_2 in solution using a K_g of 0.18 bar^{-1} .

Entry	CD	$[\text{CD}]_{\text{tot}}$ (M)	Pressure (bar)	$[\text{CD}\cdot\text{CO}_2]/[\text{CD}]_{\text{tot}}$	Time (days)	Crystal yield
1	1	0.15	6	52%	19	48%
2	1	0.15	7	56%	3	50%
3	1	0.15	10	64%	2	63%
4	1	0.15	17	75%	1	17%
5	1	0.15	20	78%	1	16%



When the crystals were treated with water, CO₂ was released as bubbles as the crystals were dissolving, which was also very clearly observed under a microscope.

To get more information about the CO₂ content in the crystal samples we also analyzed the crystals by thermogravimetric analysis. The crystal samples were heated to 26–200 °C at different rates and weight loss observed while the gas release was monitored by IR spectroscopy. Two distinguished weight decrease steps were seen in the TGA curve and very evident from the dTGA curve (Figure 3). The first weight decrease was seen around 50–75 °C and accounted for 5–6%, while the second weight decrease step normally was observed at 75–100 °C and accounts for 2–3%. IR analysis of the gas outlet showed both the characteristic water absorption at 3200–3600 cm⁻¹ and the C=O band of CO₂ at 2350 cm⁻¹ during the both weight losses but mainly CO₂ at the first lump and predominantly water at the second loss. This also suggests a comparatively weak binding of the CO₂.

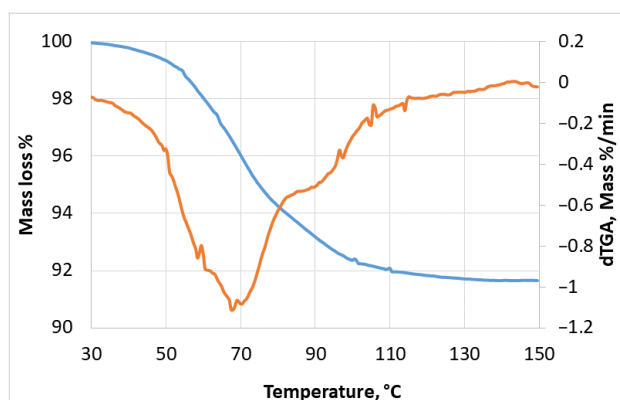


Figure 3: TGA curve (blue) and dTGA curve (red) for CO₂-1 crystals. Two lumps are seen with the former predominantly being CO₂ and the second pre-dominantly water.

We determined the binding constant for CO₂ to cyclodextrins using a pressure cell and a UV–vis competition assay with an azo-dye (4-((4-hydroxyphenyl)azo)-1-naphthalenesulfonic acid (**7**) Figure 4) [15] as an indicator. The UV–vis spectrum of **7** changes on binding to cyclodextrins and we can thereby indirectly monitor the binding of CO₂ to the CD by observing the change in spectrum of **7** provided **7** and CO₂ compete for the binding site. To avoid problems with formation of hydrogencarbonate the experiments were conducted in a buffer at pH 3 where only a minor fraction of the carbonic acid ($pK_{a1} = 3.6$) is dissociated and since the hydration constant of CO₂ is small (1.7×10^{-3}) more than 99% of CO₂ in solution is the dissolved gas at this pH. First the dissociation constants of **7**–CD complexes at pH 3, were determined (Table 2). When a solution of **7** and excess cyclodextrin was subjected to a CO₂ atmosphere at 2–8 bar in the pressure cell this gave, after equilibration for 2 hours, a change in the vis spectrum (Figure 4). The change was consistent with the displacement of **7** from the cavity by CO₂ and change in the amount of azodye was used to calculate the amount of CO₂ bound to the cyclodextrin. From the change in absorption at 370 nm as compared to the reference spectrum without cyclodextrin, we determined the gas binding constants from non-linear regression of bound CO₂ versus CO₂ pressure as shown for **1** in Figure 5. This gave the gas binding constant $K_g = [CD \cdot CO_2]/[CD]P_{CO_2}$ given in Table 2 in bar⁻¹. This constant gives the fraction of CD bound CO₂ in water under a partial pressure of CO₂. Using a literature value of the solubility of CO₂ in water at 1 bar (34 mM) and Henry's law the more traditional aqueous binding constant $K_a = [CD \cdot CO_2]/[CD][CO_2]$ in molar terms could be calculated (Table 2). For α -cyclodextrin (**1**) a K_g of 0.18 bar⁻¹ was obtained – a small value, which means that even at a partial pressure of 5 bar less than 1/2 the CD cavity is filled. The rationale for the poor binding is probably the large discrepancy between the size of CO₂ and the CD

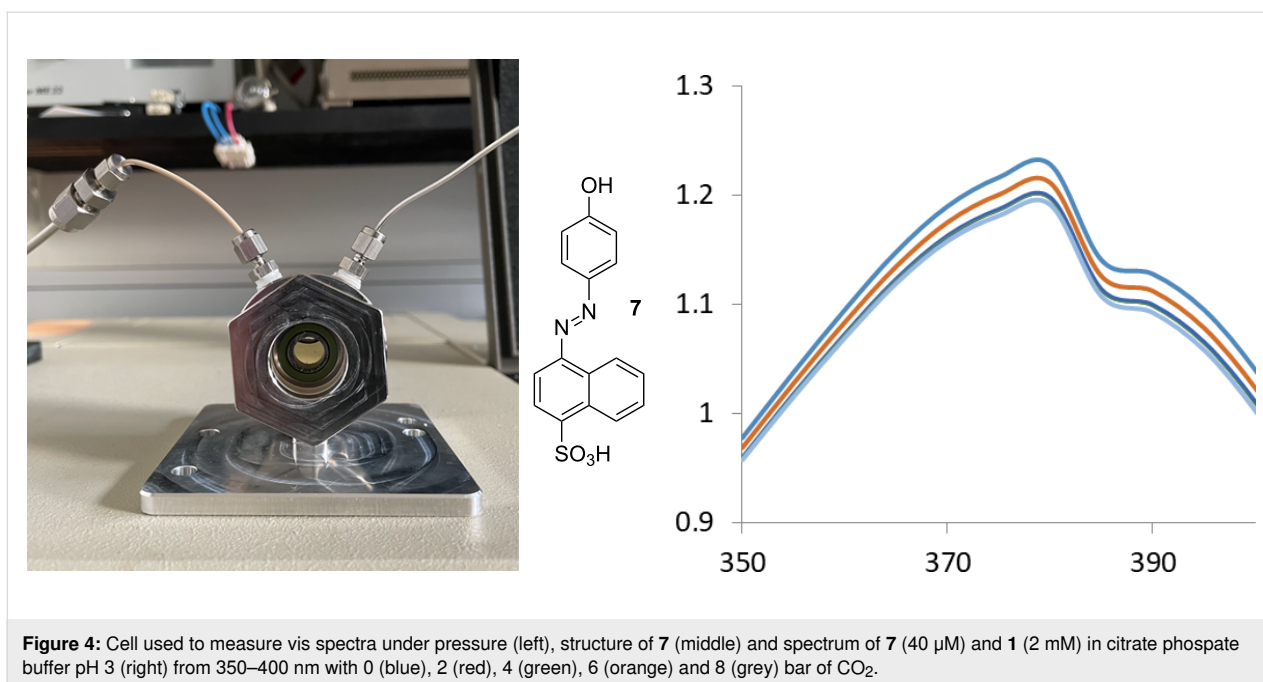


Figure 4: Cell used to measure vis spectra under pressure (left), structure of **7** (middle) and spectrum of **7** (40 μM) and **1** (2 mM) in citrate phosphate buffer pH 3 (right) from 350–400 nm with 0 (blue), 2 (red), 4 (green), 6 (orange) and 8 (grey) bar of CO_2 .

Table 2: K_d for binding of **7** and K_a for binding CO_2 for cyclodextrin derivatives in citrate-phosphate buffer at pH 3.

CD	Residues ^a	K_d of 7 at pH 3 (M)	K_g for CO_2 (bar^{-1})	K_a for CO_2 (M^{-1}) ^b	Cavity volume ^c
1 (α -CD)	6	$4.51 (\pm 1.42) \times 10^{-4}$	0.18 ± 0.02	5.3 ± 0.6	174 \AA^3
2 (β -CD)	7	$7.36 (\pm 3.16) \times 10^{-4}$	no binding	no binding	262 \AA^3
3 (γ -CD)	8	$1.63 (\pm 1.3) \times 10^{-4}$	no binding	no binding	427 \AA^3
4	6	$1.33 (\pm 0.31) \times 10^{-4}$	1.2 ± 0.14	35 ± 4.1	174 \AA^3
5	6	$2.25 (\pm 0.11) \times 10^{-3}$	0.75 ± 0.08	22 ± 2.4	155 \AA^3
6	6	$1.39 (\pm 0.25) \times 10^{-3}$	0.34 ± 0.06	9.8 ± 1.8	115 \AA^3

^aNumber of monosaccharide residues. ^bCalculated from the value in bar^{-1} by dividing with solubility of CO_2 at one bar. ^cCalculated as described by Szejtli [18].

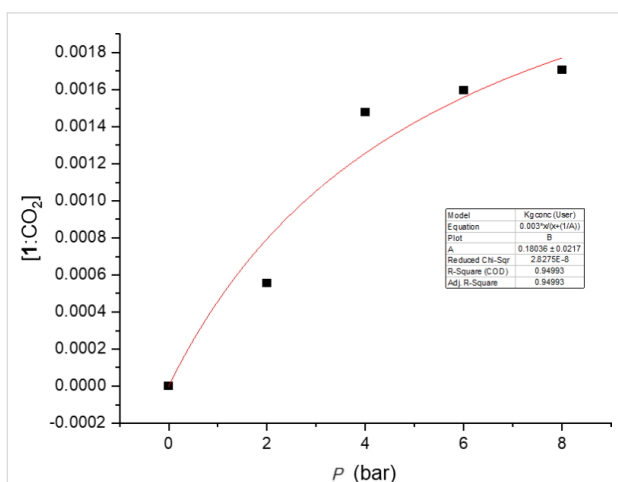


Figure 5: Binding of CO_2 to **1** as a function of pressure.

cavity. **1** has a cavity of 174 \AA^3 while CO_2 is a very small molecule with kinetic diameter of 3.3 \AA and a spherical volume of only 19 \AA^3 .

The binding for **2** and **3** and for the three derivatives of **1**, **4**, **5** and **6** were also investigated and the binding curves for determination of K_g for these derivatives are shown in Supporting Information File 1 (Figures S1–S3). The rationale for these compounds were the following:

- β - (**2**) and γ -cyclodextrins (**3**) were also studied by Cramer, but gave no crystals although they might still bind CO_2 .
- Compound **4** (permethylated α -cyclodextrin) [16] is in terms of hydrogen bonding properties and polarity vastly different from **1** yet still water-soluble.

- Compounds **5** and **6** containing 3,6-anhydrides in the α -cyclodextrin structure were chosen because they have a smaller cavity according to modelling. In models the diameter of **5** was measured and it was 5.0 Å and that of **6** was 4.6 Å with an α -CD height of 7.9 Å to give the cavity volumes given in Table 2. These compounds were made by tosylation of the corresponding partially benzylated cyclodextrins, hydrogenolysis and base treatment (see Supporting Information File 1 for experimental details). Compounds **5** and **6** have previously been made by direct tosylation of α -cyclodextrin which is a shorter route [17]. However, in our hands the direct tosylations were difficult to handle and the protection–deprotection route proved a more reliable route to pure compounds.

For **2** and **3** we found no binding which is in line with the absence of gas-crystals from these cyclodextrins. The lack of binding must, in part, be linked to the very large cavities of these molecules (Table 2). The anhydrocyclodextrins **5** and **6** have a slightly stronger binding than **1**, which on the other hand is due to these molecules having smaller cavities, although the less modified and larger monoanhydro derivative **5** was the stronger binder revealing that other factors are important. The permethylated cyclodextrin **4** was found to be the best CO₂ binder, which presumably is related to its hydrophobic character. Compound **4** is known to bind little water in the crystal (1 or 0 molecules) and probably also in solution as witnessed by its reverse temperature dependence on solubility in water [16]. Therefore, binding of the unipolar CO₂ molecule is expected to cause less water H-bond disruption in this host.

Conclusion

This work shows that CO₂ is bound 1:1 by α -cyclodextrins and that the affinity can be improved with a smaller cavity and more lipophilic cyclodextrin derivative. It suggests that stronger CO₂ binders can be found by improving on these two traits.

Experimental

Crystallization experiments. A cyclodextrin solution was prepared by dissolving **1** in Milli-Q water to the indicated concentration (Table 1). The solution was then filtered, placed in an autoclave and pressurized with CO₂ gas (pressure 6–20 bar) at 25 °C for 1–17 days. The resulting crystals were collected and filtered by suction filtration. The crystals were left to dry in a desiccator at normal pressure over CaCl₂.

X-ray analysis. The x-ray crystallographic studies were carried out on single crystals, which were coated with mineral oil, mounted on kapton loops, and transferred to the nitrogen cold stream of the diffractometer. The single-crystal X-ray diffraction studies were performed at 100(2) K on a Bruker D8

VENTURE diffractometer equipped with a Mo K α high-brilliance I μ S radiation source ($\lambda = 0.71073$ Å), a multilayer X-ray mirror and a PHOTON 100 CMOS detector, and an Oxford Cryosystems low temperature device. The instrument was controlled with the APEX3 software package using SAINT (Bruker; Bruker AXS, Inc. SAINT, Version 7.68A; Bruker AXS: Madison, WI, 2009). Final cell constants were obtained from least squares fits of several thousand strong reflections. Intensity data were corrected for absorption using intensities of redundant reflections with the program SADABS (Sheldrick, G. version 2008/2; University of Göttingen: Germany, 2003). The structures were solved in Olex2 using SHELXT and refined using SHELXL (Table 3) [19]. There is some disorder in one water molecule, which was modelled over two positions and some disorder in at least two of the primary alcohol groups, which was modelled. The latter disorder is not uncommon in

Table 3: Crystal data and structure refinement for α -CD•CO₂•5.75 H₂O.

CCDC deposition number	CCDC 2266629
empirical formula	C _{36.84} H _{69.45} O _{37.42}
formula weight	1113.90
<i>T</i> /K	100(2)
crystal system	orthorhombic
space group	<i>P</i> 2 ₁ 2 ₁ 2 ₁
<i>a</i> /Å	9.3721(6)
<i>b</i> /Å	14.3361(10)
<i>c</i> /Å	37.100(2)
α /°	90
β /°	90
γ /°	90
volume/Å ³	4984.8(6)
<i>Z</i>	4
ρ_{calc} /cm ³	1.484
μ /mm ⁻¹	0.135
<i>F</i> (000)	2365.0
crystal size/mm ³	0.244 × 0.42 × 0.28
radiation	Mo K α ($\lambda = 0.71073$)
2 θ range for data collection/°	4.35 to 61.996
index ranges	−13 ≤ <i>h</i> ≤ 13, −20 ≤ <i>k</i> ≤ 20, −47 ≤ <i>l</i> ≤ 53
reflections collected	76519
independent reflections	15881 [<i>R</i> _{int} = 0.0370, <i>R</i> _{sigma} = 0.0321]
data/restraints/parameters	15881/20/758
goodness-of-fit on <i>F</i> ²	0.993
final <i>R</i> indexes [<i>I</i> ≥ 2 σ (<i>I</i>)]	<i>R</i> ₁ = 0.0396, <i>wR</i> ₂ = 0.0966
final <i>R</i> indexes [all data]	<i>R</i> ₁ = 0.0477, <i>wR</i> ₂ = 0.1016
largest diff. peak/hole / e Å ⁻³	0.84/−0.53
Flack parameter	0.16(15)

α -cyclodextrin structures [20]. In the reported structure, CO₂ was refined with an occupancy of 0.84.

TGA measurements. These analyses were carried out on a Netzsch TG 209 F1 Libra fitted with a FTIR detector from Bruker. Samples were prepared by crushing the crystals before putting them in an aluminium crucible ensuring full coverage of the bottom. The analysis shown in Figure 3 was started at 28 °C, and was finished at a temperature of 150 °C with a heating rate of 5 °C/min.

Determination of dissociation constants between 7 and CD's. Samples were prepared that consisted of citrate-phosphate buffer (pH 3, 50 mM), 7 (40 μ M) and an increasing concentration of cyclodextrin (1–6; [CD] = 0 or 1.3–22 mM). For each sample the spectrum was recorded from $\lambda = 350$ –600 nm. For each cyclodextrin a change in the vis spectrum of 7 was seen. From Benesi–Hildebrand plots at 380 nm the K_d values given in Table 2 were found.

Determination of association constants between CD's and CO₂. Samples were prepared that consisted of citrate-phosphate buffer (pH 3, 50 mM), 7 (40 μ M) and a fixed concentration of cyclodextrin ([CD]₀; 1–4 mM) and put into the pressure cell. The spectrum was recorded at 0, 2, 4, 6 and/or 8 bar CO₂ pressure over the liquid after a 2–4 hour gas–liquid equilibration period. The K_g was determined as follows: [CD(7)] (and [7]) was calculated at each pressure from the change in absorption at 370 nm. From this [CD] was determined from the equation $K_d = [CD][7]/[CD(7)]$ and [CD(CO₂)] was calculated as $CD_{tot} - [CD] - [CD(7)]$. Now K_g was calculated by non-linear regression of [CD(CO₂)] vs P_{CO_2} as following the equation $[CD(CO_2)] = [CD]_0 P_{CO_2} / (P_{CO_2} + (1/K_g))$ as shown for 1 in Figure 5 and for 4–6 in Supporting Information File 1 (Figures S1–S3). This gave the K_g values in Table 2.

Supporting Information

Supporting Information File 1

Experimental and analytical data.

[<https://www.beilstein-journals.org/bjoc/content/supplementary/1860-5397-19-78-S1.pdf>]

Funding

800 MHz NMR data was recorded at cOpenNMR an infrastructure facility funded by the Novo Nordisk Foundation (#NNF18OC0032996). We also thank the Novo Nordisk foundation for financial support through NMR infrastructure grant (NNF21OC0067315) and project grant (NNF21OC0071886),

and the Carlsberg foundation for infrastructure grant CF21-0152.

ORCID® iDs

Heloisa Bordallo - <https://orcid.org/0000-0003-0750-0553>

Martin Jæger Pedersen - <https://orcid.org/0000-0003-3223-3661>

Mikael Bols - <https://orcid.org/0000-0002-6561-6952>

References

- Keeling, C. D. *Annu. Rev. Energy Environ.* **1998**, *23*, 25–82. doi:10.1146/annurev.energy.23.1.25
- Lüthi, D.; Le Floch, M.; Bereiter, B.; Blunier, T.; Barnola, J.-M.; Siegenthaler, U.; Raynaud, D.; Jouzel, J.; Fischer, H.; Kawamura, K.; Stocker, T. F. *Nature* **2008**, *453*, 379–382. doi:10.1038/nature06949
- Evans, J. *Elements of a Sustainable World*; Oxford University Press, 2020. doi:10.1093/oso/9780198827832.001.0001
- Klaus, S.; Lehenmeier, M. W.; Anderson, C. E.; Rieger, B. *Coord. Chem. Rev.* **2011**, *255*, 1460–1479. doi:10.1016/j.ccr.2010.12.002
- Ohno, H.; Ikhlayel, M.; Tamura, M.; Nakao, K.; Suzuki, K.; Morita, K.; Kato, Y.; Tomishige, K.; Fukushima, Y. *Green Chem.* **2021**, *23*, 457–469. doi:10.1039/d0gc03349a
- Albero, J.; Peng, Y.; Garcia, H. *ACS Catal.* **2020**, *10*, 5734–5749. doi:10.1021/acscatal.0c00478
- Panja, P.; McPherson, B.; Deo, M. *Carbon Capture Sci. Technol.* **2022**, *3*, 100041. doi:10.1016/j.ccst.2022.100041
- Cramer, F.; Henglein, F. M. *Chem. Ber.* **1957**, *90*, 2572–2575. doi:10.1002/cber.19570901123
- Li, H.; Zhang, B.; Li, C.; Fu, X.; Wang, Z.; Huang, Q. *Food Chem.* **2019**, *289*, 145–151. doi:10.1016/j.foodchem.2019.03.037
- Ho, T. M.; Howes, T.; Bhandari, B. R. *Food Chem.* **2015**, *187*, 407–415. doi:10.1016/j.foodchem.2015.04.094
- Ho, T. M.; Howes, T.; Bhandari, B. R. *J. Food Process. Preserv.* **2018**, *42*, e13514. doi:10.1111/jfpp.13514
- Eftaiha, A. F.; Qaroush, A. K.; Alsoubani, F.; Pehl, T. M.; Troll, C.; Rieger, B.; Al-Maythaly, B. A.; Assaf, K. I. *RSC Adv.* **2018**, *8*, 37757–37764. doi:10.1039/c8ra08040b
- Manor, P. C.; Saenger, W. *J. Am. Chem. Soc.* **1974**, *96*, 3630–3639. doi:10.1021/ja00818a042
- Saenger, W.; Noltemeyer, M. *Chem. Ber.* **1976**, *109*, 503–517. doi:10.1002/cber.19761090214
- Cramer, F.; Saenger, W.; Spatz, H.-C. *J. Am. Chem. Soc.* **1967**, *89*, 14–20. doi:10.1021/ja00977a003
- Steiner, T.; Saenger, W. *Carbohydr. Res.* **1996**, *282*, 53–63. doi:10.1016/0008-6215(95)00364-9
- Fujita, K.; Tahara, T.; Egashira, Y.; Yamamura, H.; Imoto, T.; Koga, T.; Fujioka, T.; Mihashi, K. *Chem. Lett.* **1988**, *17*, 705–708. doi:10.1246/cl.1988.705
- Szejtli, J. *Chem. Rev.* **1998**, *98*, 1743–1754. doi:10.1021/cr970022c
- Sheldrick, G. M. *Acta Crystallogr., Sect. A: Found. Crystallogr.* **2008**, *64*, 112–122. doi:10.1107/s0108767307043930
- Aree, T.; Jacob, J.; Saenger, W.; Hoier, H. *Carbohydr. Res.* **1998**, *307*, 191–197. doi:10.1016/s0008-6215(97)10109-4

License and Terms

This is an open access article licensed under the terms of the Beilstein-Institut Open Access License Agreement (<https://www.beilstein-journals.org/bjoc/terms>), which is identical to the Creative Commons Attribution 4.0 International License (<https://creativecommons.org/licenses/by/4.0>). The reuse of material under this license requires that the author(s), source and license are credited. Third-party material in this article could be subject to other licenses (typically indicated in the credit line), and in this case, users are required to obtain permission from the license holder to reuse the material.

The definitive version of this article is the electronic one which can be found at:
<https://doi.org/10.3762/bjoc.19.78>